Available online at www.eccomasproceedia.org
Eccomas Proceedia COMPDYN (2017) 3963-3981

ECCOMAS
Proceedia

COMPDYN 2017
6th ECCOMAS Thematic Conference on
Computational Methods in Structural Dynamics and Earthquake Engineering
M. Papadrakakis, M. Fragiadakis (eds.)
Rhodes Island, Greece, 15–17 June 2017

OPTIMAL FRICTION COEFFICIENTS FOR ISOLATED STRUCTURES DEPENDING ON THE SOIL CONDITION

P. Castaldo[1] and M. Ripani[2]

[1]Department of Structural, Geotechnical and Building Engineering (DISEG), Politecnico di Torino, Corso Duca degli Abruzzi, 24, Turin, Italy (corresponding author);
e-mail: paolo.castaldo@polito.it; pcastaldo@unisa.it

[2]CONICET-National Scientific and Technical Research Council, Materials and Structures Laboratory, University of Buenos Aires, Argentina;
e-mail: mripani@fi.uba.ar

Keywords: seismic isolation; friction pendulum isolators; performance-based engineering; non-dimensional form; optimal isolator properties; power spectral density method; soil condition.

Abstract. *This study aims at evaluating the optimal properties of friction pendulum bearings to be employed for the seismic protection of elastic isolated structural systems under earthquake excitations with different characteristics in terms of frequency content. A two-degree-of-freedom model is considered to describe the isolated system behavior while accounting for the superstructure flexibility and a non-dimensional formulation of the governing equations of motion is employed to relate the characteristic parameters describing the isolator and structure properties to the response parameters of interest for the performance assessment. Seismic excitations are modelled as time-modulated filtered Gaussian white noise random processes of different intensity within the power spectral density method. The filter parameters control the frequency content of the random excitations and are calibrated to describe stiff, medium and soft soil conditions, respectively. Finally, multi-variate regression expressions are obtained for the optimum values of the friction coefficient that minimize the superstructure displacements relative to the base mass as a function of the structural system properties, of the seismic input intensity and of the soil condition.*

Peer-review under responsibility of the organizing committee of COMPDYN 2017.
doi: 10.7712/120117.5697.16854

1 INTRODUCTION

Over the years, within the issue of the passive control of structures, many works have developed new design strategies and methodologies [1]-[4]. Isolation systems have emerged as a very effective technique for seismic protection of building frames [5]. Friction pendulum system (FPS) bearings are often preferred to other types of bearings due to their capability of providing an isolation period independent of the mass of the supported structure, their high dissipation and recentering capacity, and their longevity and durability characteristics [6]-[7]. Many experimental and numerical studies have been carried out to investigate the behavior of these devices and to define reliable models for describing it [8]-[13]. Other studies have focused on the seismic response of structures isolated with FPS bearings by accounting for the variability of the seismic input characteristics [14]-[16]. In [17] the influence of friction pendulum system (FPS) isolator properties on the seismic performance of base-isolated building frames was investigated by employing a two-degree-of-freedom model accounting for the superstructure flexibility with a velocity-dependent model for the FPS isolator behaviour. The variation of the statistics of the response parameters relevant to the seismic performance has been investigated through the nondimensionalization of the motion equation considering different isolator and system properties.

Other works (e.g. [18]-[25]) have been more oriented to develop design approaches for the isolators and to identify the optimal isolator properties. In this context, Castaldo et al. [18]-[19] proposed a seismic reliability-based design (SRBD) criterion to define the isolator dimensions in plan based on the evaluation of performance curves for the isolator and the superstructure. Bucher [25] proposed a reliability-based design approach for the bearings accounting for the probabilistic performance properties in terms of maximum and residual isolator displacements, and the maximum interstorey structural displacement. Jangid [21]-[22], considering a stochastic model of the earthquake ground motion, evaluated the seismic performance of a single shear type building isolated by FPS bearings whose behavior was described by a Coulomb model showing that there exists an optimal value of the friction coefficient for which the top floor absolute acceleration of the building is minimized. This value is influenced by the building properties and the isolation period, and it increases with the increase of the earthquake intensity. The minimization of the absolute accelerations of the isolated superstructure was employed as optimization criterion also in other works [23]-[24]. In [26], considering a ten-story shear type building as case study, a multi-objective optimization for the optimal design of sliding isolation systems for suppression of seismic responses of building structures is presented applying a genetic algorithm to minimize the building's top story displacement, its acceleration and also the base raft's displacement.

As for the effect of the frequency characteristics and its influence on the seismic response of base-isolated systems and on the optimal isolator properties, other studies (e.g., [27]-[29]), concerning isolated buildings and bridges, demonstrated that soft soil condition leads to a great alteration of the variances with large increment of the peak ratios, in terms of displacements and shear forces, by negatively affecting the isolated systems. Similarly, Kulkarni and Jangid [30] analyzed the effects of superstructure flexibility on the response of base-isolated structures subjected to non-stationary random processes by comparing the stochastic response of a base-isolated structure with superstructure modelled as flexible and rigid and highlighting that the seismic isolation is more effective for firm or rock type soil than the soft soils.

This work aims to investigate the influence of soil characteristics in terms of frequency content on the seismic performance of elastic building frames isolated with FPS isolators and the optimal isolator friction properties. The two-degree-of-freedom model, already employed in [17], is used for this purpose, as it was shown to provide a reliable representation of the

structural response of more complex systems, especially in the case of low values of the friction coefficient and high isolation degrees such that the effects of the higher modes are negligible. It is also useful because it leads to a condensed description of the problem in terms of few characteristic parameters representing the isolator and structural system properties. A parametric study of the system is performed for different values of these characteristic parameters by considering three different sets of artificial ground motion records, modelled as non-stationary stochastic processes and generated through the power spectral density method [31], with different frequency content corresponding to stiff, medium and soft soil conditions [32], respectively. The nondimensionalization of the governing equations of motions permits to investigate wide ranges of seismic intensities while limiting the required nonlinear response history analyses. For each set of random excitations, numerical simulations are first carried out to evaluate the relation between the characteristic system and isolator parameters and the structural performance. Successively, multi-variate regression expressions are derived for the optimal values of the friction coefficient that minimize the superstructure displacements relative to the base, as a function of the system characteristic parameters, of the seismic input intensity and of the soil condition. More details may be found in [33].

2 NON-DIMENSIONAL EQUATION OF MOTION

The equations of motion governing the response of a 2dof model representing an elastic system on single concave FPS isolation bearings (Fig. 1) subjected to the seismic input $\ddot{u}_g(t)$, in the hypothesis of considering the horizontal component of the bearings displacement, is:

$$\begin{aligned} &m_s\ddot{u}_s(t)+c_s\dot{u}_s(t)+k_s u_s(t)=-m_s\left[\ddot{u}_g(t)+\ddot{u}_b(t)\right] \\ &m_b\ddot{u}_b(t)+f_b(t)+c_b\dot{u}_b(t)-c_s\dot{u}_s(t)-k_s u_s(t)=-m_b\ddot{u}_g(t) \end{aligned} \tag{1}$$

where u_s denotes the displacement of the superstructure relative to isolation bearing, u_b the isolator displacement relative to the ground, m_s and m_b respectively the mass of the superstructure and of the base floor above the isolation system, k_s and c_s respectively the superstructure stiffness and inherent viscous damping constant, c_b the bearing viscous damping constant, t the time instant, the dot differentiation over time, and $f_b(t)$ denotes the FPS bearing resisting force. This latter can be expressed as:

$$f_b(t)=k_b u_b(t)+\mu(\dot{u}_b)(m+m_b)gZ(t) \tag{2}$$

where $k_b=W/R=(m_s+m_b)g/R$, g is the gravity constant, R is the radius of curvature of the FPS, $\mu(\dot{u}_b(t))$ the coefficient of sliding friction, which depends on the bearing slip velocity $\dot{u}_b(t)$, and $Z(t)=\mathrm{sgn}(\dot{u}_b)$, with $sgn(\cdot)$ denoting the sign function. The fundamental period of vibration of a base-isolated system, $T_b=2\pi\sqrt{R/g}$, corresponding to the pendulum component, is independent of the superstructure mass and related only to the radius of curvature R [17].

Experimental results [9]-[11] suggest that the coefficient of sliding friction of Teflon-steel interfaces obeys to the following equation:

$$\mu(\dot{u}_b)=f_{\max}-Df\cdot\exp\left(-\alpha|\dot{u}_b|\right) \tag{3}$$

in which $f_{\max}$ represents the maximum value of friction coefficient attained at large velocities of sliding, and $f_{\min} = f_{\max} - Df$ represents the value at zero velocity. In this study, to further simplify the problem, it is assumed that $f_{\max} = 3f_{\min}$ with the exponent α equal to 30 [17].

Moreover, note that, in the hypothesis of considering the maximum value of the sliding friction coefficient, it is possible to evaluate the effective stiffness of the isolation level $k_{eff} = W\left(1/R + f_{\max}/u_b\right)$ depending on the bearings displacement (Fig. 1) which leads to an effective isolated period $T_{b,eff}$ [34],[35].

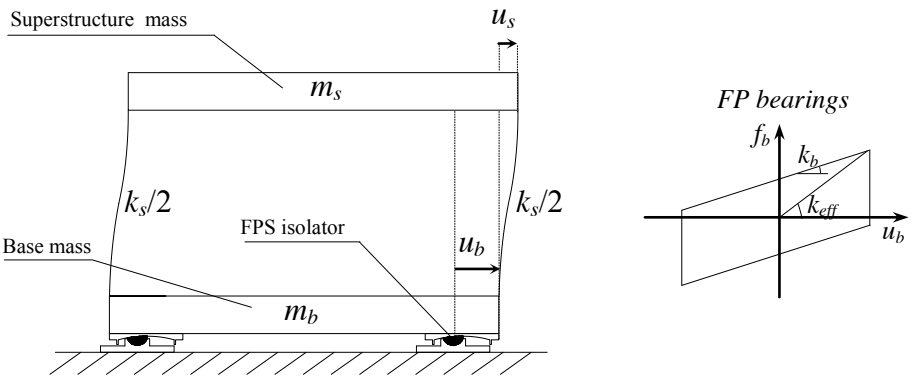

Fig. 1. 2dof model of elastic system isolated with FPS in the deformed configuration.

The non-dimensional form of the equations of motion can be derived by introducing the time scale $\tau = t\omega_b$, where $\omega_b = \sqrt{k_b/\left(m_s + m_b\right)}$ denotes the fundamental circular frequency of the isolated system with infinitely rigid superstructure, and the seismic intensity scale a_0, which has the dimension of an acceleration and it is such that $\ddot{u}_g(t) = a_0\lambda(\tau)$, where $\lambda(\tau)$ is a non-dimensional function of time describing the seismic input time-history. In [17], the following non-dimensional equations are obtained:

$$\begin{aligned}
&\ddot{\psi}_s(\tau) + 2\xi_s\frac{\omega_s}{\omega_b}\dot{\psi}_s(\tau) + \frac{\omega_s^2}{\omega_b^2}\psi_s(\tau) = -\left[\lambda(\tau) + \ddot{\psi}_b(\tau)\right] \\
&\ddot{\psi}_b(\tau) + \frac{1}{1-\gamma}\left[2\xi_b\dot{\psi}_b(\tau) + \psi_b(\tau) + \frac{\mu\left(\dot{u}_b\right)g}{a_0}\operatorname{sgn}\left(\dot{\psi}_b\right)\right] - 2\xi_s\frac{\omega_s}{\omega_b}\frac{\gamma}{1-\gamma}\dot{\psi}_s(\tau) - \frac{\omega_s^2}{\omega_b^2}\frac{\gamma}{1-\gamma}\psi_s(\tau) = -\lambda(\tau)
\end{aligned} \tag{4}$$

where $\omega_s = \sqrt{k_s/m_s}$ and $\xi_s = c_s/2m_s\omega_s$ denote respectively the circular frequency and damping factor of the superstructure; $\xi_b = c_b/2m_b\omega_b$ the isolator damping factor; $\gamma = m_s/\left(m_s + m_b\right)$ [34] the mass ratio. The non-dimensional parameters $\psi_s = u_s\omega_b^2/a_0$ and $\psi_b = u_b\omega_b^2/a_0$ describe the dynamic response of the superstructure and the isolators respectively. Eqn.(4) also reveals that the non-dimensional parameters (Π terms) [36]-[37] that control the system non-dimensional response to the seismic input $\lambda(\tau)$ are:

$$\Pi_\omega = \frac{\omega_s}{\omega_b}, \Pi_\gamma = \gamma, \Pi_\mu\left(\dot{\psi}_b\right) = \frac{\mu\left(\dot{u}_b\right)g}{a_0}, \Pi_{\xi_b} = \xi_b, \Pi_{\xi_s} = \xi_s \tag{5}$$

Parameter Π_ω measures the isolation degree [34],[38], Π_γ is the previously defined mass ratio, Π_{ξ_b} and Π_{ξ_s} describe the viscous damping inherent respectively to the system and the isolator. The non-dimensional parameter Π_μ measures the isolator strength, provided by the friction coefficient $\mu(\dot{u}_b)$, relative to the seismic intensity. Since this parameter depends on the response through the velocity $\dot{u}_b$, the following parameter is used in its stead:

$$\Pi_\mu^* = \frac{f_{\max} g}{a_0} \tag{6}$$

It is noteworthy that the non-dimensional seismic response of the system does not depend on the seismic intensity level a_0, but it depends only on $\Pi_{\xi_b}, \Pi_{\xi_s}, \Pi_\omega, \Pi_\gamma, \Pi_\mu^*$, and on the function $\lambda(\tau)$, describing the frequency content and time-modulation of the seismic input. Moreover, having assumed $1/\omega_b$ as time scale, it follows that also ω_b influences the non-dimensional seismic response of the system [17].

3 PARAMETRIC STUDY

This section presents the results of the parametric study carried out on the system of Fig. 1 to evaluate the performance of elastic buildings isolated with FPS bearings for different structural properties and soil conditions. The first two subsections describe respectively the stochastic model employed to generate the random excitations and the response parameters used to monitor the seismic performance, whereas the final subsection shows the parametric study results.

3.1 Random excitations and intensity measure (*IM*)

In Eqn.(4), the seismic input is described by the intensity scale factor, a_0, which is commonly denoted to as seismic intensity measure (*IM)* in the context of the performance-based earthquake engineering (PBEE) [39],[40], and through the non-dimensional function $\lambda(\tau)$, which describes the time-history of the ground motions.

The "record-to-record" variability of the characteristics of the seismic inputs is herein described by defining three wide sets of artificial record time histories with different frequency content corresponding to stiff, medium and soft soil conditions, respectively. These artificial records are modelled as time-modulated filtered Gaussian white noise random processes [30],[31],[41]. The power spectral density (PSD) function [42] of the embedded stationary process is described by the widely-used Kanai-Tajimi model [43]-[44], as modified by Clough and Penzien [45],[29],[46]-[50], i.e.:

$$S_f(\omega) = \frac{\omega_g^4 + 4\xi_g^2\omega_g^2\omega^2}{(\omega_g^2 - \omega^2) + 4\xi_g^2\omega_g^2\omega^2} \cdot \frac{\omega^4}{(\omega_f^2 - \omega^2) + 4\xi_f^2\omega_f^2\omega^2} S_0 \tag{7}$$

where S_0 = amplitude of the bedrock excitation spectrum, modeled as a white noise process; ω_g and ξ_g = fundamental circular frequency and damping factor of the soil, respectively; ω_f and ξ_f = parameters describing the Clough-Penzien filter; and ω = the circular frequency ranging between 0 and 50 rad/s. The parameters ω_g and ξ_g are assumed as uniformly distributed independent random variables, with the following ranges of variation [32],[51]:

ω_g=5π-9π (high frequency/short period) and ξ_g=0.6-1 for stiff soil condition, ω_g=3π-5π (intermediate frequency/ period) and ξ_g=0.4-0.6 for medium soil condition, ω_g=π-3π (low frequency/high period) and ξ_g=0.2-0.4 for soft soil condition. The values of the Clough-Penzien filter parameters are assumed as deterministic and equal to $\omega_f = 1.6$ (rad/s) and $\xi_f = 0.6$.

The Shinozuka-Sato function [52] is used to modulate in time the embedded stationary processes, Eqn.(8):

$$I(t) = c \cdot (e^{-b_1 \cdot t} - e^{-b_2 \cdot t}) \tag{8}$$

where b_1= 0.045π s^{-1}, b_2= 0.050π s^{-1} and c=25.302. A duration equal to 31.25 s, longer than 25s according to [53], is considered. The same duration has been assumed for all the artificial record time histories since the duration of the random excitations has not a strong influence when a peak response quantity is of interest, like the maximum response displacement, velocity or acceleration [54],[55].

An ensemble of 100 artificial ground motions, generated through the Spectral Representation Method [31], is considered for each soil condition. By this way, each set of artificial records reflects the wide uncertainty in terms of frequency content related to each soil condition [32],[51] and is composed of a high number of random excitations in order to strongly reduce the standard errors [16] of the statistics of the response parameters evaluated in the following subsections.

Fig. 2(a) shows the PSD functions for the different soil conditions corresponding to S_0=1 m^2/s^3 and to the sample values of the filter parameters, illustrating the energy associated with the frequency contents for each soil condition [56], whereas, Fig. 2(b) shows the elastic pseudo-acceleration response spectra of the 100 artificial ground motions for each soil condition, scaled to the common *IM* value $S_A(T)$ = 0.1 g, for T = 4 s, which is a typical isolated system period.

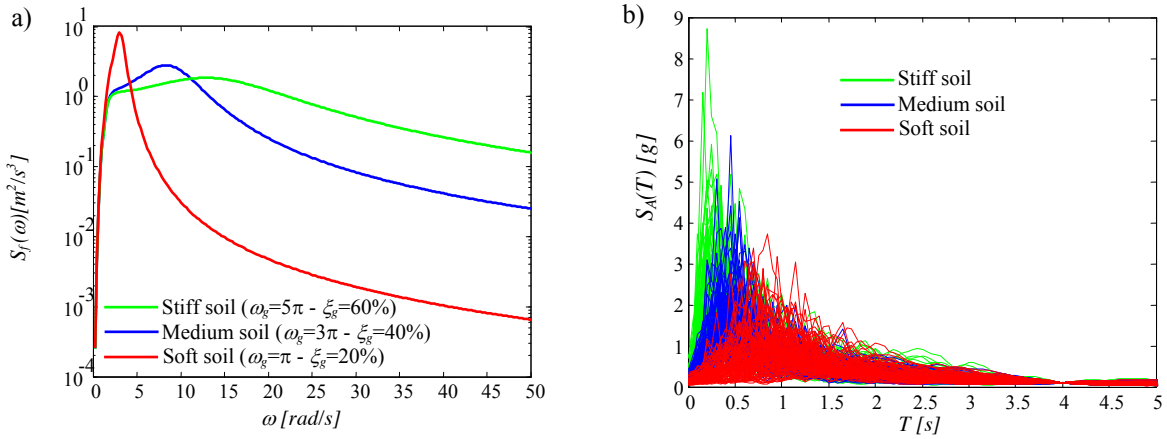

Fig. 2. PSD functions corresponding to stiff, medium and soft soil conditions (a); Pseudo-acceleration response spectra for the 300 records scaled to the common seismic intensity measure $S_A(T)$ = 0.1 g, for T=4s (b).

Regarding the intensity measure, it is worth to note that although the non-dimensional response to a single ground motion input does not depend on the *IM* level a_0, the response dispersion, and thus the accuracy of the estimate, is affected by the *IM* choice [17]. In this study, the spectral pseudo-acceleration, $S_A(T_b, \xi_b)$, at the isolated period of the system, $T_b = 2\pi / \omega_b$, and for the damping ratio $\Pi_{\xi_b} = \xi_b$, is assumed as *IM*. This *IM* is related to the spectral displacement S_d by the relation $S_A(T_b, \xi_b) = \omega_b^2 S_d(T_b, \xi_b)$. It is also worth to observe that if all

the records for each soil type are normalized to $S_A\left(T_b,\xi_b\right)$, then the normalized displacement response of a system with period T_b, damping ratio ξ_b, rigid superstructure (i.e., high Π_ω) and mounted on a frictionless isolator, equals to 1 for each record and soil condition and it is not affected by the record-to-record variability. Thus, this system can be assumed as reference case for evaluating the influence of the isolator friction Π_μ and of the period ratio Π_ω on the response statistics [17]. In the analyses carried out in this study, the damping ratio ξ_b is taken equal to zero, consistently with other works which assume that friction is the only source of damping in the isolators [17],[22],[57]. The corresponding *IM* is hereinafter denoted to as $S_A\left(T_b\right)$.

3.2 Seismic response parameters

This study considers the following set of response parameters relevant to the performance of the isolated system: the peak isolator displacement $u_{b,\max}$ (important for the design of the FPS isolator and of the seismic gap around the building), the peak superstructure displacement relative to the isolator $u_{s,\max}$ (related to internal forces in the structure and to the performance of displacement-sensitive non-structural components). These response parameters can be expressed in non-dimensional form, according to Eqn. (4), as:

$$\psi_{u_b}=\frac{u_{b,\max}\omega_b^2}{S_A\left(T_b\right)}=\frac{u_{b,\max}}{S_d\left(T_b\right)} \quad , \quad \psi_{u_s}=\frac{u_{s,\max}\omega_b^2}{S_A\left(T_b\right)}=\frac{u_{s,\max}}{S_d\left(T_b\right)} \tag{9a,b}$$

where the normalized displacement response ψ_{u_b} can be interpreted as the reduction factor of the response spectrum at the isolation period T_b with damping ratio ξ_b=0.

By repeatedly solving Eqn. (4) for each set of the 100 ground motion records, a set of samples is obtained for the output variables used to monitor the performance. In this paper, the response parameters are assumed to follow a lognormal distribution [17]-[18],[39],[57]-[58]. The lognormality assumption permits to estimate, with a limited number of samples, the response at different percentile levels, which is very useful for system reliability assessment. It also permits to obtain a closed-form analytical estimate of the seismic risk [59].

A lognormal distribution can be fitted to the generic response parameter *D* (i.e., the extreme values ψ_{u_b},ψ_{u_s} of Eq. (4)) by estimating the sample geometric mean, $GM\left(D\right)$, and the sample lognormal standard deviation $\sigma_{\ln}\left(D\right)$, or dispersion $\beta\left(D\right)$, defined, respectively, as follows:

$$GM\left(D\right)=\sqrt[N]{d_1\cdot\ldots\cdot d_N} \tag{10}$$

$$\beta\left(D\right)=\sigma_{\ln}\left(D\right)=\sqrt{\frac{\left(\ln d_1-\ln\left[GM\left(D\right)\right]\right)^2+\ldots\ldots+\left(\ln d_N-\ln\left[GM\left(D\right)\right]\right)^2}{N-1}} \tag{11}$$

where d_i denotes the *i*-th sample value of *D*, and *N* is the total number of samples. The sample geometric mean is an estimator of the median of the response and its logarithm coincides with the lognormal sample mean $\mu_{\ln}\left(D\right)$. Under the lognormality assumption, the relation between the geometric mean $GM\left(D\right)$, the dispersion $\beta\left(D\right)$, and the *k*th percentile of the generic response parameter *D* can be expressed as:

$$d_k = GM(D)\exp[f(k)\beta(D)] \tag{12}$$

where $f(k)$ is a function assuming the values $f(50)=0$, $f(84)=1$ and $f(16)=-1$ [60].

3.3 Parametric study results

This section shows the results of the parametric study carried out to evaluate the relation between the isolation and structure properties and the system performance, for each set of 100 ground motion records corresponding to different soil conditions. The parameters $\Pi_{\xi_b}=\xi_b$ and $\Pi_{\xi_s}=\xi_s$ are assumed respectively equal to 0% and 2%, the base-isolated system period T_b is varied in the range between 2s and 5s, the parameter Π_ω in the range between 3 (flexible superstructure) and 12 (rigid superstructure), $\Pi_\gamma=\gamma$ in the range between 0.6 and 0.9, Π_μ^* in the range between 0 (no friction) and 2 (very high friction). Indeed, a high value for the upper bound of Π_μ^* is also considered due to the very low values of the *IM* at high isolated periods (i.e., T_b=5s) depending on the seismic hazard [53]. For each value of the parameters varied in the parametric study, the differential equation of motion, i.e., Eqn.(4), has been repeatedly solved for the different random excitation. The Bogacki-Shampine integration algorithm available in Matlab-Simulink [61] has been employed. The probabilistic properties of the normalized response have been evaluated by estimating the geometric mean, *GM*, and the dispersion, β, of the parameters of interest through Eqns. (10) and (11).

Figs. 3-8 show the statistics (*GM* and β values) of the response parameters considered, obtained for different values of the system parameters varying in the range of interest and for each soil type. Each figure contains several surface plots, corresponding to different values of Π_γ. Only the results corresponding to Π_ω = 6 and Π_ω = 9 are reported.

Fig.s 3 and 4 plot the results concerning the normalized bearing displacement ψ_{u_b}, related to cases Π_ω=6 and Π_ω=9 respectively. The trend of $GM\left(\psi_{u_b}\right)$ is similar to that discussed in [17], where natural records were considered without taking into account soil types.

This is the consequence of the non-dimensionalization and of the efficient intensity measure employed for the study. In fact, $GM\left(\psi_{u_b}\right)$ is equal to unit for $\Pi_\mu^*=0$ and higher Π_ω and increases slightly for increasing T_b because of period elongation and of the influence of the second mode of vibration on the response. Obviously, $GM\left(\psi_{u_b}\right)$ decreases significantly as Π_μ^* increases and is also slightly influenced by Π_γ, especially, for low Π_ω values. For soft soil condition and low Π_ω values, the influence of Π_γ is higher as well as the decrease of $GM\left(\psi_{u_b}\right)$ for increasing Π_μ^* is more gradual. The dispersion $\beta\left(\psi_{u_b}\right)$ for high T_b increases for increasing values of Π_μ^*, as a result of the reduction of the efficiency of the *IM* employed in the study for each soil condition. Moreover, with reference to soft soils, the values of $\beta\left(\psi_{u_b}\right)$ also result to be higher for low values of both the isolated periods T_b and Π_μ^*. Obviously, in the case of $\Pi_\mu^*=0$ and higher Π_ω, the dispersion is zero for all the values of T_b and of Π_γ considered and for all the soil conditions.

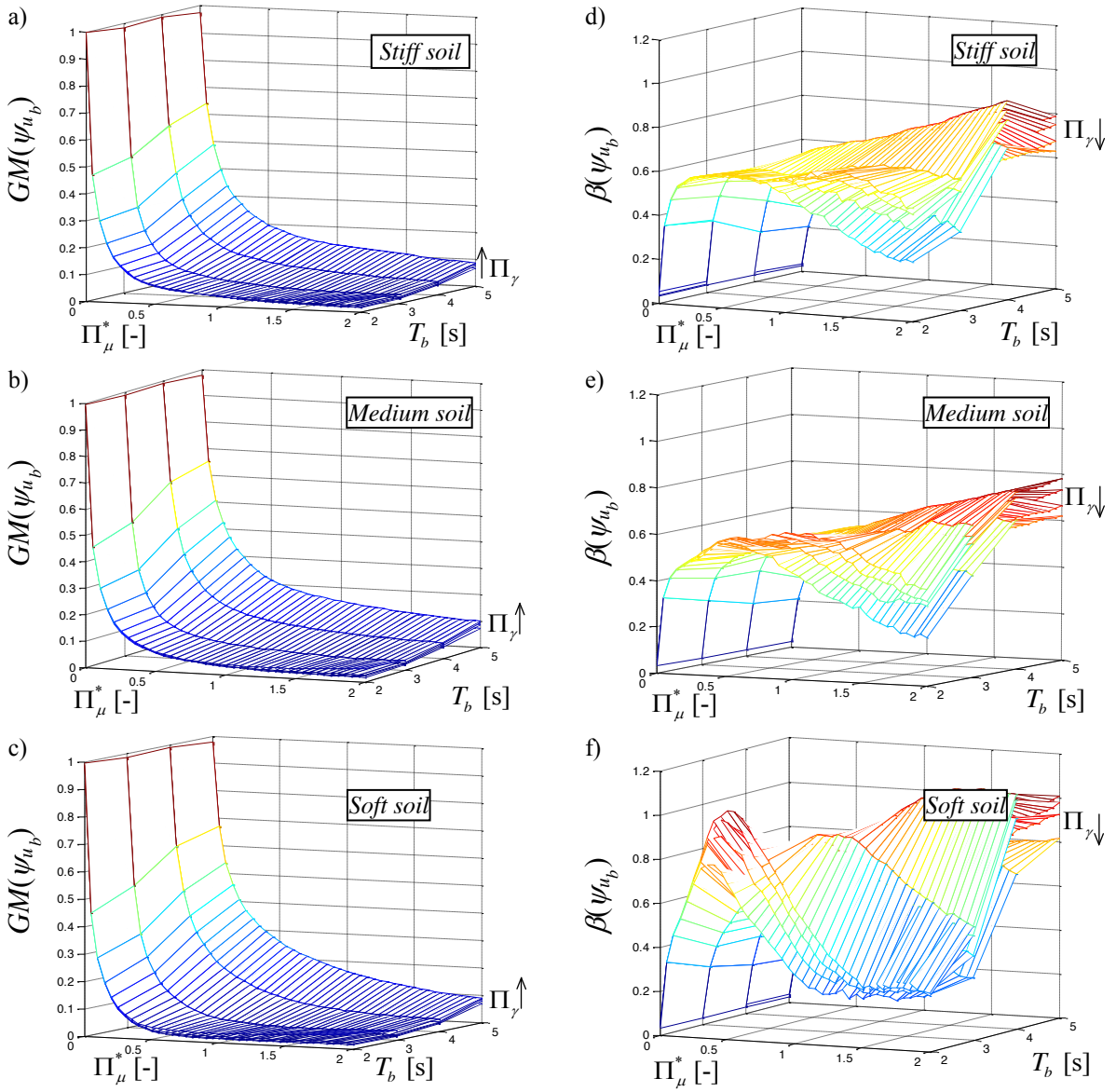

Fig. 3. Normalized bearing displacement vs. Π^*_μ and T_b for Π_ω=6 and each soil condition: median value (a,b,c) and dispersion (d,e,f) for different values of Π_γ. The arrow denotes the increasing direction of Π_γ.

The mass ratio Π_γ does not affect significantly the response dispersion, especially in the case of high Π_ω values. The above described peak values of both $GM\left(\psi_{u_b}\right)$ and $\beta\left(\psi_{u_b}\right)$ in the case of soft soil condition are due to resonance effects which mainly affect the effective frequency charactering the dynamic behaviour of the frictional bearings and the dominant frequency of the corresponding random excitations.

Fig.s 5 and 6 show the response statistics of the normalized superstructure displacements relative to the base mass ψ_{u_s}. Also the trend of $GM\left(\psi_{u_s}\right)$ is quite similar to that discussed in [17]: $GM\left(\psi_{u_s}\right)$ increases for increasing values of T_b as well as for decreasing values of Π_γ and of Π_ω, whereas it first decreases and then increases for increasing values of Π^*_μ. Thus, there exists an optimal value of Π^*_μ such that the superstructure displacement is minimized

for each soil condition. This optimal value is in the range between 0 and 0.3 depending on the values of Π_ω, T_b, Π_γ and soil condition. In particular, increasing values of the optimal friction coefficient are required from stiff to soft soil condition.

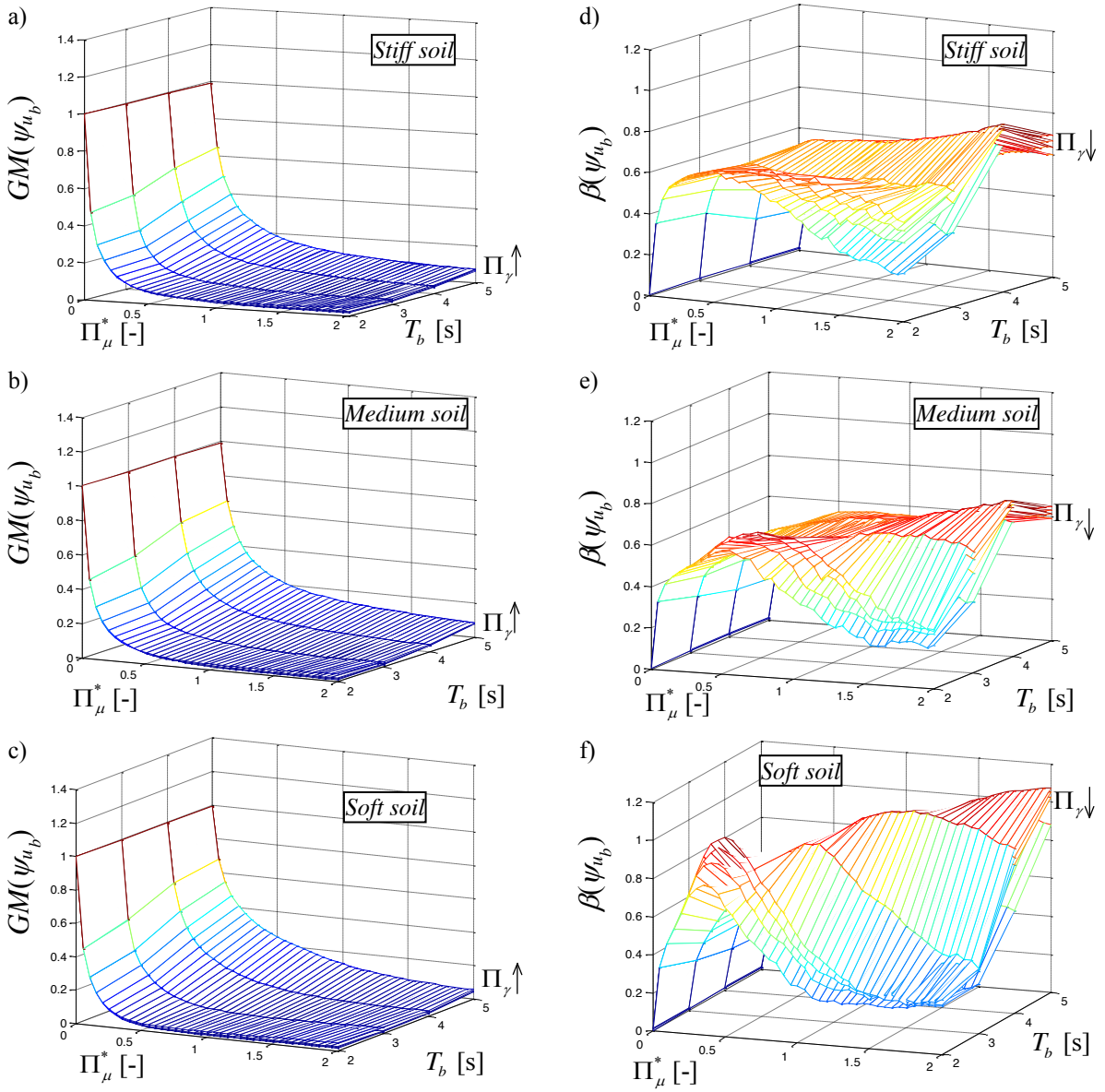

Fig. 4. Normalized bearing displacement vs. Π^*_μ and T_b for Π_ω=9 and each soil type: median value (a,b,c) and dispersion (d,e,f) for different values of Π_γ. The arrow denotes the increasing direction of Π_γ.

The values of the dispersion $\beta(\psi_{u_s})$, are very low for low Π^*_μ values due to the high efficiency of the *IM* employed in the study, and attain their peak for values of Π^*_μ close to the optimal ones. The other system parameters have a reduced influence on $\beta(\psi_{u_s})$ compared to the influence of Π^*_μ. In the case of soft soil condition, the dispersion $\beta(\psi_{u_s})$ strongly increases for increasing values of Π^*_μ for both lower isolation degrees and isolated periods because of the resonance effects which mainly affect the effective frequency of the frictional bearings and the dominant frequency of the corresponding random excitations. The different

influence of the three soil conditions and, in particular, the increase of the statistics values of the response parameters from stiff to soft soil condition results to be consistent with the results described in [28]-[30].

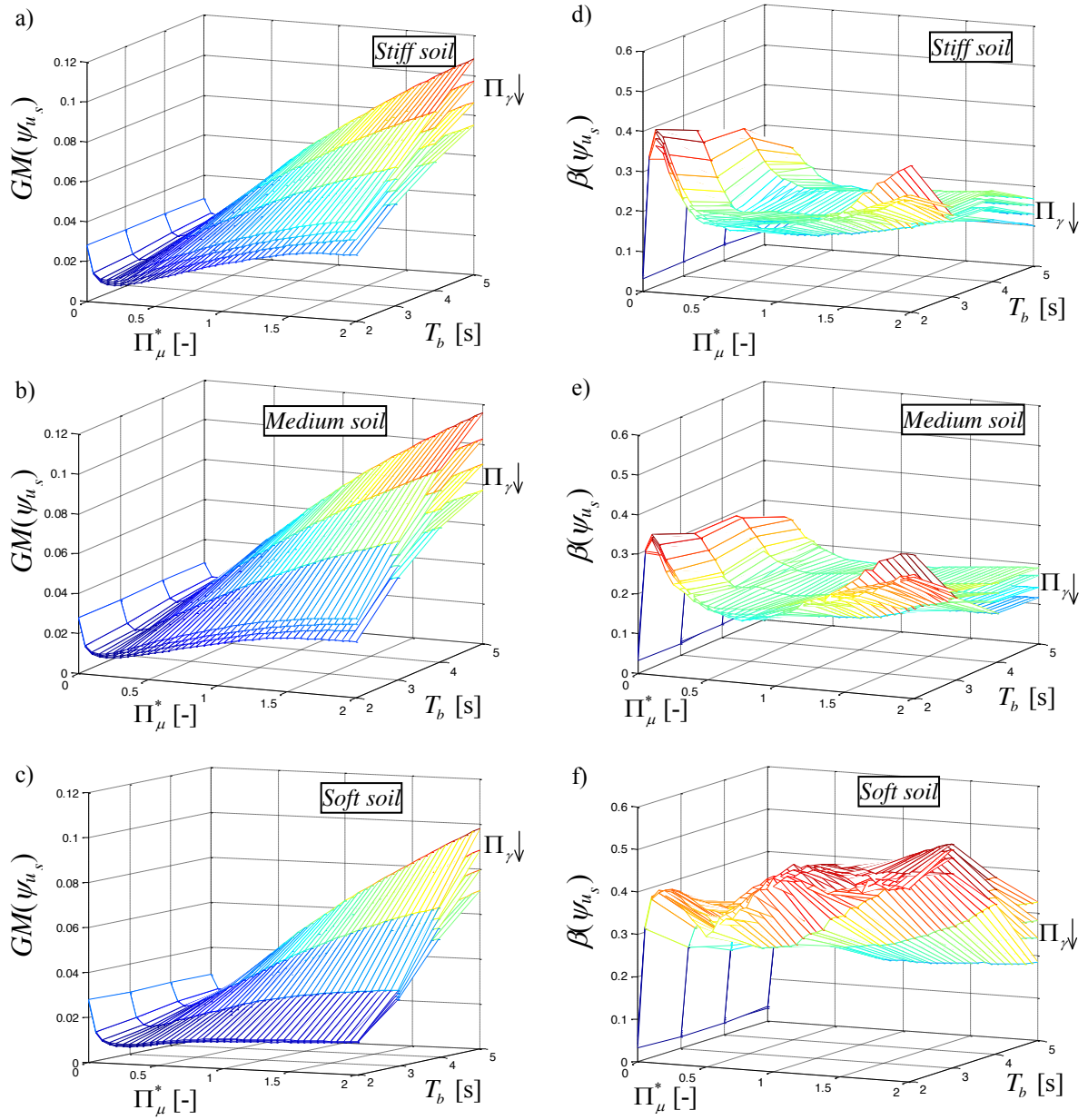

Fig. 5. Normalized superstructure displacement vs. Π^*_μ and T_b for Π_ω=6 and each soil condition: median value (a,b,c) and dispersion (d,e,f) for different values of Π_γ. The arrow denotes the increasing direction of Π_γ.

The existence of an optimal value of the friction coefficient has been pointed out in many studies on systems isolated by FPS bearings [17],[21]-[24],[26] and it depends on some effects that follow an increase of the friction coefficient. In fact, an increase of the friction coefficient leads to an increase of the isolator strength (and thus of the equivalent stiffness, with a reduction of the corresponding effective fundamental vibration period (Fig.1)) and the increase of participation of higher vibration modes as well as transfer of forces towards the superstructure. However, the forces transmitted to the superstructure also depend on the bearings displacements which decrease as the friction coefficient increases. An increase of the forces transmitted to the superstructure generally increases the superstructure displacements.

Another effect is an increase of energy dissipation (equivalent damping), which reduces the superstructure displacements. The equilibrium between these effects is strongly influenced by the characteristic structural parameters as well as the frequency content of the random excitations related to each soil condition. In fact, for soft soil condition, higher optimal values of the normalised friction coefficient are required due to the resonance effects as well as to increase the equivalent damping. The dependency on these parameters is discussed in more detail in the next section.

For all the statistics of the response parameters within the parametric analysis, the standard errors [16] result to be lower than 5% for low values of Π_{μ}^{*} and lower than 10% for increasing values of Π_{μ}^{*} due to the high number of the random excitations employed.

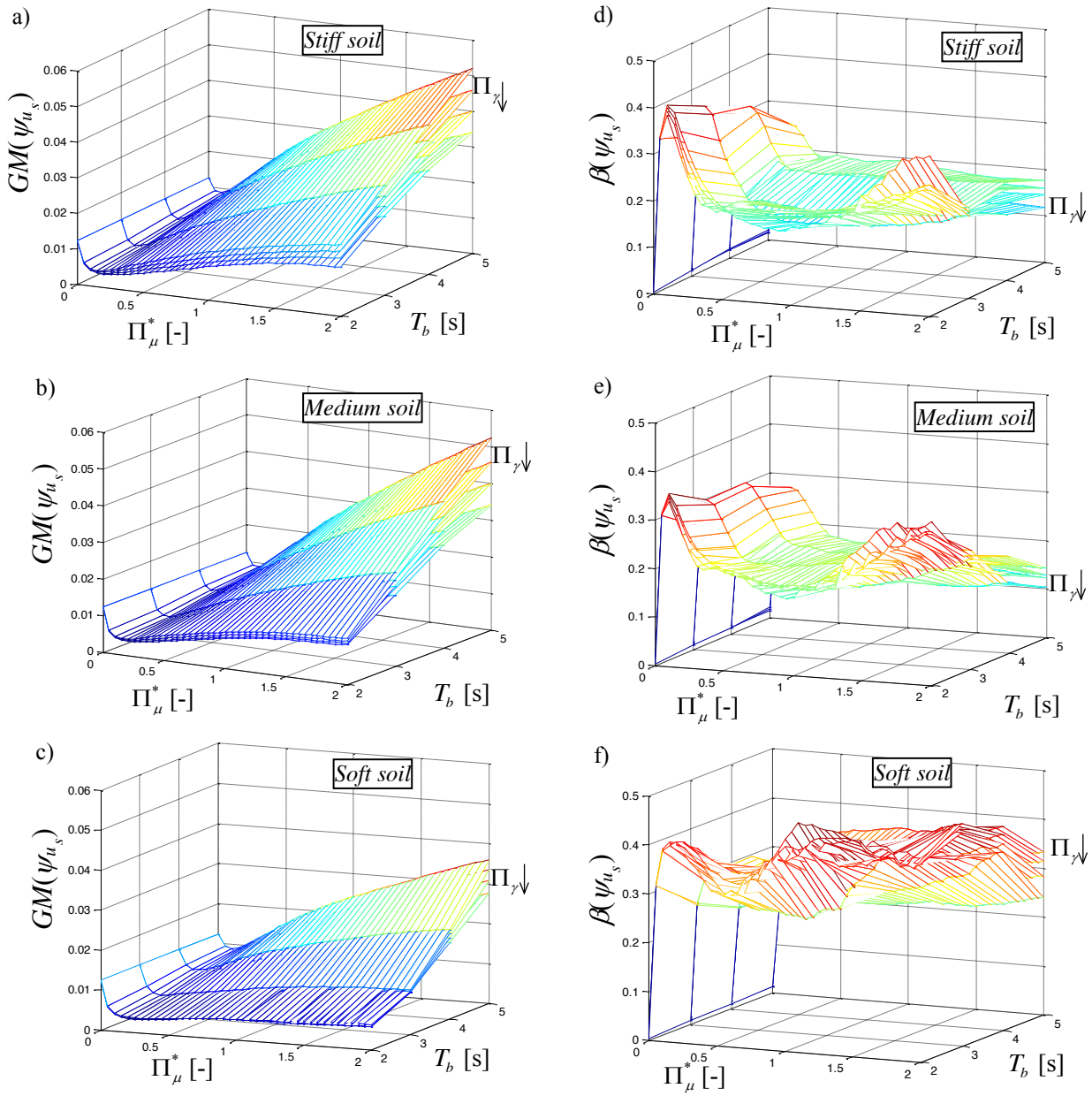

Fig. 6. Normalized superstructure displacement vs. Π^{*}_{μ} and T_b for Π_{ω}=9 and each soil condition: median value (a,b,c) and dispersion (d,e,f) for different values of Π_{γ}. The arrow denotes the increasing direction of Π_{γ}.

4 OPTIMAL SLIDING FRICTION COEFFICIENT DEPENDING ON THE SOIL CONDITION

The results previously described show that for each combination of the system properties (i.e., of Π_γ, T_b and Π_ω) there exists an optimal value of the normalized sliding friction coefficient, $\Pi^*_{\mu,\text{opt}}$, depending on the soil condition such that the median normalized superstructure displacements are minimized according to Fig.s 5-6.

Minimizing the superstructure displacements relative to the base mass can be an important design requirement for base isolated systems to avoid inelastic response of the superstructure, which can lead to very high displacement ductility demand [62]. In fact, an inelastic response of the superstructure can lead to a disproportionately large displacement ductility demand that could also be amplified in the case of soft soil condition due to the resonance effects, considering structural systems in ordinary conditions and neglecting aging effects [63]-[72].

From a design point of view, it may be of interest to evaluate the values of $\Pi^*_{\mu,\text{opt}}$ that minimize response percentile others than the 50$^{\text{th}}$, corresponding to different exceedance probabilities [57]. Therefore, for each soil type, through a multivariate nonlinear regression analysis, a regression expression is obtained for $\Pi^*_{\mu,\text{opt}}$ as a function of the parameters Π_γ, T_b and Π_ω and of three percentile levels (i.e., 50$^{\text{th}}$, 16$^{\text{th}}$ and 84$^{\text{th}}$ percentiles). In particular, the expressions for $\Pi^*_{\mu,opt}$ is derived by fitting in Matlab [61] the following second-order polynomial expression:

$$\begin{aligned}\Pi^*_{\mu,\text{opt}} &= c_1 + c_2\cdot T_b + c_3\cdot\Pi_\omega + c_4\cdot\Pi_\gamma + c_5\cdot T_b\cdot\Pi_\omega + c_6\cdot T_b\cdot\Pi_\gamma + \\ &+ c_7\cdot\Pi_\gamma\cdot\Pi_\omega + c_8\cdot {T_b}^2 + c_9\cdot {\Pi_\omega}^2 + c_{10}\cdot {\Pi_\gamma}^2\end{aligned} \tag{13}$$

where c_i, i=1,…,10, are the regression coefficients, whose values are reported in Tables 1-3 as a function of the different percentile levels and soil condition. It is noteworthy that the order of the polynomials is kept as small as possible to balance the contrasting requirements of accuracy and simplicity, thus providing a polynomial expression easy to be applied for the preliminary designing of FPS characteristics.

	c_1	c_2	c_3	c_4	c_5	c_6	c_7	c_8	c_9	c_{10}
50$^{\text{th}}$ percentile	0.2657	-0.0380	-0.0083	-0.2022	-0.0012	-0.0028	0.0071	0.0045	0.0005	0.2187
84$^{\text{th}}$ percentile	0.2643	-0.0249	-0.0034	-0.2641	-0.0016	-0.0126	0.0044	0.0020	0.0005	0.3359
16$^{\text{th}}$ percentile	0.3038	-0.0392	-0.0083	-0.3230	-0.0010	0.0181	0.0034	0.0037	0.0005	0.2422

Table 1. Coefficients of multi-variate non-linear regression for stiff soil.

	c_1	c_2	c_3	c_4	c_5	c_6	c_7	c_8	c_9	c_{10}
50$^{\text{th}}$ percentile	0.2248	-0.0327	-0.0034	-0.1122	-0.0007	0.0162	0.0059	0.0008	0.0002	0.1094
84$^{\text{th}}$ percentile	0.1973	0.0055	-0.0064	-0.1456	-0.0011	0.0090	0.0080	-0.0055	0.0005	0.1719
16$^{\text{th}}$ percentile	0.2483	-0.0376	-0.0058	-0.1906	-0.0011	0.0301	0.0049	0.0020	0.0005	0.1172

Table 2. Coefficients of multi-variate non-linear regression for medium soil.

The regression R-squared values are higher than 0.92 for all the cases considered, indicating that the fitted model describes well the variation of $\Pi^*_{\mu,opt}$ with the parameters considered. Only the regressions, related to the 16th percentile for stiff and medium soil conditions, present slightly lower values of R-squared. Eqn. (13) can be used to design the optimum FPS properties for the isolated system, provided that a seismic intensity level $S_A(T_b)$ is assigned. In fact, according to Eqn. (6), the optimum friction coefficient (at high velocity) can be easily calculated as $f_{\max,\text{opt}} = \dfrac{\Pi^*_{\mu,\text{opt}} \cdot S_A(T_b)}{g}$. This implies that the optimum friction coefficient increases linearly with the *IM* level. Furthermore, friction pendulum properties that are "optimal" for a given seismic intensity, are not "optimal" for the other intensities. It follows that the optimal friction coefficient can be defined considering the seismic intensity corresponding to the collapse limit state [53] in order to ensure an adequate response of the isolated superstructure under strong earthquake events. More details may be found in [33].

	c_1	c_2	c_3	c_4	c_5	c_6	c_7	c_8	c_9	c_{10}
50th percentile	0.5689	-0.1603	0.0113	-0.4345	-0.0005	0.0632	0.0007	0.0108	-0.0003	0.2187
84th percentile	0.3726	-0.0629	0.0204	-0.4317	-0.0018	0.0292	-0.0038	0.0008	-0.0004	0.3437
16th percentile	0.5751	-0.1607	0.0022	-0.3256	0.0002	0.0665	0.0079	0.0103	-0.0004	0.0781

Table 3. Coefficients of multi-variate non-linear regression for soft soil.

5 CONCLUSIONS

This paper investigates the influence of the soil characteristics in terms of frequency content, related to stiff, medium and soft soils, on the seismic performance of elastic buildings isolated with friction pendulum system (FPS) bearings and the optimal isolator friction properties. In particular, the results of an extensive parametric study, encompassing a wide range of isolator and building properties, different seismic intensity levels, different soil conditions and various response parameters that are of interest for monitoring the seismic behavior, are described. The behavior of these systems is analyzed by employing a two-degree-of-freedom model accounting for the superstructure flexibility, whereas the FPS isolator behaviour is described by adopting a widespread model which considers the variation of the friction coefficient with the velocity.

The uncertainty in the seismic inputs is taken into account by considering for each (stiff, medium and soft) soil condition a set of 100 artificial records, obtained through the power spectral density method, with different frequency content and scaled to increasing intensity levels. A nondimensionalization of the equation of motion is carried out to unveil the parameters controlling the problem and also allows to explore a wide range of situations while limiting the required nonlinear response history analyses. The estimates of the response statistics obtained for each combination of the parameters reflect the effect of the variability of the frequency characteristics of the seismic input at different intensity levels and can be used for deriving approximate fragility curves and for simplified seismic risk analyses.

For each set of random excitations, the influence of superstructure and FPS system properties are evaluated by considering the geometric mean (*GM*) and dispersion of each normalised response parameter, assumed to follow a lognormal distribution. With reference to both isolation device and superstructures response, it is possible to conclude that low-frequency random excitations related to soft soil condition negatively influences the statistics of the response pa-

rameters of the whole isolated systems due to resonance effects which affect seismic inputs dominant frequencies and the effective frequency of the frictional bearings.

Finally, multi-variate regression expressions are derived for the optimal values of the normalized friction coefficient minimizing the 50^{th}, 16^{th} and 84^{th} percentile values of the superstructure displacements relative to the base mass, as function of the identified system characteristic parameters and soil type. Thus the performance of both the structural and non-structural components of the superstructure can be controlled. Higher values of the optimum friction coefficient are required, especially for low isolated periods, in the case of soft soil condition in order to reduce the bearing displacements and, consequently, the forces transmitted to the superstructure as well as to increase the energy dissipation (equivalent damping).

REFERENCES

[1] De Iuliis M., Castaldo P., Palazzo B., Analisi della domanda sismica inelastica del terremoto de L'Aquila su sistemi dimensionati secondo le NTC2008. *Ingegneria Sismica*, Patron Editore **XXVII**(3), 55–68, 2010.

[2] Castaldo, P., Palazzo, B., Perri F. FEM simulations of a new hysteretic damper: the dissipative column, *Ingegneria Sismica - International Journal of Earthquake Engineering*, Anno XXXIII – Speciale CTA- 2015- Num. 1-2:34-45.

[3] Castaldo P., *Integrated Seismic Design of Structure and Control Systems*. Springer International Publishing: New York, 2014 . DOI 10.1007/978-3-319-02615-2.

[4] De Iuliis M., Castaldo P., An energy-based approach to the seismic control of one-way asymmetrical structural systems using semi-active devices, *Ingegneria Sismica - International Journal of Earthquake Engineering* **XXIX**(4):31-42, 2012.

[5] Christopoulos C, Filiatrault A. *Principles of Passive Supplemental Damping and Seismic Isolation*. IUSS Press: Pavia, Italy, 2006.

[6] Su L, Ahmadi G, Tadjbakhsh IG. Comparative study of base isolation systems. *Journal of Engineering Mechanic* 1989; **115**(9):1976–92.

[7] Zayas VA, Low SS, Mahin SA. A simple pendulum technique for achieving seismic isolation. *Earthquake Spectra* 1990; **6**(2):317–33.

[8] Mosqueda G, Whittaker AS, Fenves GL. Characterization and modeling of Friction Pendulum bearings subjected to multiple components of excitation. *Journal of Structural Engineering* 2004; **130**(3):433-442.

[9] Mokha A, Constantinou MC, Reinhorn AM. Teflon Bearings in Base Isolation. I: Testing. *Journal of Structural Engineering* 1990; **116**(2):438-454.

[10] Constantinou MC, Mokha A, Reinhorn AM. Teflon Bearings in Base Isolation. II: Modeling. *Journal of Structural Engineering* 1990; **116**(2):455-474.

[11] Constantinou MC, Whittaker AS, Kalpakidis Y, Fenz DM, Warn GP. Performance of Seismic Isolation Hardware Under Service and Seismic Loading. *Technical Report* MCEER-07-0012, 2007.

[12] Almazàn JL, De la Llera JC. Physical model for dynamic analysis of structures with FPS isolators. *Earthquake Engineering and Structural Dynamics* 2003;**32**(8):1157–1184.

[13] Landi, L, Grazi G, and Diotallevi P P. Comparison of different models for friction pendulum isolators in structures subjected to horizontal and vertical ground motions, *Soil Dynamics and Earthquake Engineering* 2016;**81**:75-83.

[14] Ryan KL, Chopra AK. Estimating the seismic displacement of friction pendulum isolators based on non-linear response history analysis. *Earthquake Engineering and Structural Dynamics* 2004;**33**(3):359–373.

[15] Barroso LR. Performance evaluation of vibration controlled steel structures under seismic loads. PhD thesis, Stanford University, California, US, 1999.

[16] Barroso LR, Winterstein S. Probabilistic seismic demand analysis of controlled steel moment-resisting frame structures. *Earthquake Engineering and Structural Dynamics* 2002;**31**(12):2049–2066.

[17] Castaldo, P, Tubaldi, E. Influence of FPS bearing properties on the seismic performance of base-isolated structures. *Earthquake Engineering and Structural Dynamics* 2015;**44**(15):2817–2836.

[18] Castaldo P., Amendola G., Palazzo B., Seismic fragility and reliability of structures isolated by friction pendulum devices: seismic reliability-based design (SRBD), *Earthquake Engineering and Structural Dynamics*, **46**(3); 425–446, 2017, DOI: 10.1002/eqe.2798.

[19] Castaldo P., Palazzo B. and Ferrentino T. Seismic reliability-based ductility demand evaluation for inelastic base-isolated structures with friction pendulum devices, Earthquake Engineering and Structural Dynamics 2017; 46:1245–1266, DOI: 10.1002/eqe.2854.

[20] Castaldo, P., Amendola, G., Palazzo, B. Effetcs of class B site on the seismic reliability of base-isolated steel systems, Ingegneria Sismica, **33**(3), 29-41, 2015.

[21] Jangid RS. Optimum frictional elements in sliding isolation systems. *Computers and Structures* 2000;**76**(5):651–661.

[22] Jangid RS. Optimum friction pendulum system for near-fault motions. *Engineering Structures* 2005;**27**(3):349-359.

[23] Chung LL, Kao PS, Yang CY, Wu LY, Chen HM. Optimal frictional coefficient of structural isolation system. *Journal of Vibration and Control* 2013, Early view. DOI: 10.1177/1077546313487938.

[24] Iemura H, Taghikhany T, Jain S. Optimum design of resilient sliding isolation system for seismic protection of equipments. *Bulletin of Earthquake Engineering* 2007;**5**(1):85-103.

[25] Bucher C. Probability-based optimization of friction-based seismic isolation devices. *Structural Safety* 2009;**31**(6):500-507.

[26] Fallah, N., Zamiri G. Multi-objective optimal design of sliding base isolation using genetic algorithm. *Scientia Iranica A*, 2013;**20**(1):87–96.

[27] Dicleli, M., & Buddaram, S. Effect of isolator and ground motion characteristics on the performance of seismic-isolated bridges. *Earthquake Engineering and Structural Dynamics* 2006;**35**(2):233-250.

[28] Safak, E., Frankel, A. Effects of ground motion characteristics on the response of base-isolated structures. *11th World Conference on Earthquake Engineering 1996* (paper no. 1430).

[29] Saritaş, F, Hasgür Z. Dynamic Behavior of an Isolated Bridge Pier under Earthquake Effects for Different Soil layers and Support Conditions, *Digest* 2014, 1733-1756.

[30] Kulkarni JA, Jangid RS. Effects of superstructure flexibility on the response of base-isolated structures. Shock and Vibration 2003;26:1-13.

[31] Shinozuka M., Deodatis G. Simulation of stochastic processes by spectral representation. *Applied Mechanics Reviews* 1991;**44**(4):191-203.

[32] Pinto P, Giannini R, Franchin P. Seismic Reliability Analysis of Structures. *Iuss Press* 2004.

[33] Castaldo P., Ripani M. Optimal design of friction pendulum system properties for isolated structures considering different soil conditions. *Soil Dynamics and Earthquake Engineering*; 90:74 – 87, 2016. DOI:10.1016/j.soildyn.2016.08.025.

[34] Kelly JM. *Earthquake-Resistant Design with Rubber*. 2nd ed. Berlin and New York: Springer-Verlag; 1997.

[35] Building Seismic Safety Council. NEHRP Recommended Provisions: Design Examples FEMA 451 - Washington, D.C., August 2006.

[36] Karavasilis TL, Seo CY, Makris N. Dimensional Response Analysis of Bilinear Systems Subjected to Non-pulse like Earthquake Ground Motions. *Journal of Structural Engineering* 2011;**137**(5):600-606.

[37] Barbato M, and Tubaldi E. A probabilistic performance-based approach for mitigating the seismic pounding risk between adjacent buildings. *Earthquake Engineering & Structural Dynamics* 2013;**42**(8):1203-1219.

[38] Palazzo B. Seismic Behavior of base-isolated Buildings. Proceedings of the International Meeting on earthquake Protection of Buildings, Ancona, 1991.

[39] Aslani H, Miranda E. Probability-based seismic response analysis. *Engineering Structures* 2005;**27**(8):1151-1163.

[40] Porter KA. An overview of PEER's performance-based earthquake engineering methodology. Proceedings, *Proceedings of the 9th International Conference on Application of Statistics and Probability in Civil Engineering* (*ICASP9*), San Francisco, California, 2003.

[41] Pradlwarter H. J., SchuiRler G. I., Dorka U. Reliability of MDOF-systems with hysteretic devices. *Engineering Structures*, 1998;**20**(8):685-691.

[42] Tung ATY, Wang JN, Kiremidjian A, Kavazanjian E. Statistical parameters of AM and PSD functions for the generation of site-specific strong ground motions. Proceedings *of the 10th World Conference on Earthquake Engineering*, Madrid, Spain, 1992;**2**:867-872.

[43] Kanai K. Semiempirical formula for the seismic characteristics of the ground. *Bulletin of earthquake research institute* 1957;**35**:309-325.

[44] Tajimi H. A statistical method of determining the maximum response of a building structure during an earthquake. *Proc., 2nd World Conf. on earthquake Engineering* 1960;**II**:781-798.

[45] Clough R.W., Penzien J.: Dynamics of Structures, 2nd edn. McGraw-Hill, New York; 1993.

[46] Zentner I., Allain F., Humbert N., Caudron M. Generation of spectrum compatible ground motion and its use in regulatory and performance-based seismic analysis. *Proceedings of the 9th Internat. Conf. on Str. Dyn.s*, EURODYN 2014 Porto, Portugal, 30 June - 2 July 2014.

[47] Peng Y., Chen J., Li J. Nonlinear Response of Structures Subjected to Stochastic Excitations via Probability Density Evolution Method. *Advances in Structural Engineering*, 2014;**17**(6):801-816.

[48] Li, C., Liu, Y. Ground Motion Dominant Frequency Effect On The Design Of Multiple Tuned Mass Dampers. *Journal of Earthquake Engineering*, 2004;**8**(1):89-105.

[49] Lopez-Garcia, D., Soong T.T. Assessment of the separation necessary to prevent seismic pounding between linear structural systems. *Prob. Engineering Mechanics*, 2009;**24**:210-223.

[50] Tubaldi, E., Barbato, M., Ghazizadeh S. A probabilistic performance-based risk assessment approach for seismic pounding with efficient application to linear systems. *Structural Safety* 2012;36-37:14–22.

[51] Talaslidis D.G., Manolis G.D., Paraskevopoulos E.A., Panagiotopoulos C.G. Risk analysis of industrial structures with hazardous materials under seismic input, 13th World Conference on Earthquake Engineering, Vancouver, B.C., Canada, August 1-6, 2004.

[52] Shinozuka M, Sato Y. Simulation of nonstationary random process. *J. Engrg. Mech. Div*. 1967;**93**(1):11-40.

[53] NTC08. Norme tecniche per le costruzioni. Gazzetta Ufficiale del 04.02.08, DM 14.01.08, Ministero delle Infrastrutture.

[54] Hancock J, Bommer JJ. A state-of-knowledge review of the influence of strong- motion duration on structural damage. *Earthquake Spectra* 2006;**22**(3):827-845.

[55] Hancock J, Bommer JJ. Using spectral matched records to explore the influence of strong-motion duration on inelastic structural response. *Soil Dynamics and Earthquake Engineering* 2007;**27**:291-299.

[56] Armouti, N.S. Response of structures to synthetic earthquakes. *Emerging Technologies in Structural Engineering. Proc. of the 9th Arab Structural Engineering Conf.*, Nov. 29 – Dec. 1, 2003, Abu Dhabi, UAE, 331-340.

[57] Ryan K, Chopra A. Estimation of Seismic Demands on Isolators Based on Nonlinear Analysis. *Journal of Structural Engineering* 2004;**130**(3):392-402.

[58] Karavasilis T, Seo C. Seismic structural and non-structural performance evaluation of highly damped self-centering and conventional systems. *Eng. Structures* 2011,**33**(8):2248-2258.

[59] Cornell C, Jalayer F, Hamburger R, Foutch D. Probabilistic Basis for 2000 SAC Federal Emergency Management Agency Steel Moment Frame Guidelines. *Journal of Structural Engineering* 2002;**128**(4):526-533.

[60] Ang AHS, Tang WH. Probability Concepts in Engineering-Emphasis on Applications to Civil and Environmental Engineering. John Wiley & Sons, New York, USA; 2007.

[61] Math Works Inc. MATLAB-High Performance Numeric Computation and Visualization Software. User's Guide. Natick: MA, USA; 1997.

[62] Vassiliou F M, Tsiavos A, Stojadinović B. Dynamics of inelastic base-isolated structures subjected to analytical pulse ground motions. *Earth.Eng.& Str. Dyn.*, 2013;**42**(14):2043-2060.

[63] Castaldo, P., Palazzo, B., Mariniello, A.. Effects of the axial force eccentricity on the time-variant structural reliability of aging r.c. cross-sections subjected to chloride-induced corrosion Engineering Structures, **130**: 261-274, 2017.

[64] Palazzo, B., Castaldo, P., Mariniello, A. Time-variant structural reliability of R.C. structures affected by chloride-induced deterioration, American Concrete Institute, ACI Special Publication 2015-January (SP 305), pp. 19.1-19.10

[65] Etse, G.J., Ripani, M., Vrech, S.M. "Fracture energy-based thermodynamically consistent gradient model for concrete under high temperature," Proceedings of the 8th International Conference on Fracture Mechanics of Concrete and Concrete Structures, FraMCoS 2013, 1506-1515.

[66] Etse, G., Ripani, M., Caggiano, A. & Schicchi, D.S. "Strength and durability of concrete subjected to high temperature: continuous and discrete constitutive approaches," American Concrete Institute, ACI Special Publication 2015-January (SP 305), 9.1-9.18.

[67] Etse, G., Ripani, M. & Mroginski, J.L. "Computational failure analysis of concrete under high temperature," Computational Modelling of Concrete Structures - Proceedings of EURO-C 2014, 2:715-722.

[68] Etse, G., Vrech, S.M. & Ripani, M. "Constitutive theory for Recycled Aggregate Concretes subjected to high temperature," Construction and Building Materials; **111**: 43-53, 2016.

[69] Mroginski, J.L., Etse, G., Ripani, M. "A non-isothermal consolidation model for gradient-based poroplasticity," PANACM 2015 - 1st Pan-American Congress on Computational Mechanics, in conjunction with the 11th Argentine Congress on Computational Mechanics, MECOM 2015, pp. 75-88.

[70] Ripani, M., Etse, G., Vrech, S. & Mroginski, J.L. "Thermodynamic gradient-based poroplastic theory for concrete under high temperature," International Journal of Plasticity; **61**: 157-177, 2014.

[71] Ripani, M., Etse, G., Vrech, S. "Recycled aggregate concrete: localized failure assessment in thermodynamically consistent non-local plasticity framework", Computers and Structures, **178**: 47–57, 2017, doi: 10.1016/j.compstruc.2016.08.007.

[72] Vrech, S.M., Ripani, M. & Etse, G. "Localized versus diffused failure modes in concrete subjected to high temperature," PANACM 2015 - 1st Pan-American Congress on Computational Mechanics, in conjunction with the 11th Argentine Congress on Computational Mechanics, MECOM 2015, pp. 225-236.